R. & M. No. 2781
(12,387)
A.R.C. Technical Report

MINISTRY OF SUPPLY

AERONAUTICAL RESEARCH COUNCIL
REPORTS AND MEMORANDA

The 9 x 3 in. Induced-flow High-speed Wind Tunnel at the National Physical Laboratory

By

D. W. HOLDER, D.I.C., A.C.G.I., B.Sc., and R. J. NORTH,
of the Aerodynamics Division, N.P.L.

LONDON: HER MAJESTY'S STATIONERY OFFICE
1953
EIGHT SHILLINGS NET

The 9 x 3 in. Induced-flow High-Speed Wind Tunnel at the National Physical Laboratory

By

D. W. HOLDER, D.I.C., A.C.G.I., B.Sc., and R. J. NORTH
of the Aerodynamics Division, N.P.L.

Reports and Memoranda No. 2781*

June, 1949

Summary.—A 9 × 3 in. high-speed wind tunnel driven by a compressed-air injector has been built in the Aerodynamics Division of the National Physical Laboratory. The tunnel operates at roughly atmospheric stagnation pressure and has so far been used to give Mach numbers up to 1·8. The general arrangement of the tunnel and the preliminary calibration, which is generally satisfactory, are described.

1. *Introduction.*—It was proposed[1] to construct two 36 × 12 in. high-speed wind tunnels on the West Aero. site at the National Physical Laboratory†. Both were intended primarily for two-dimensional experiments; one for flutter work, and the other to augment the facilities provided by the existing 20 × 8 in. tunnel (R. & M. 2067[2]) for testing aerofoil sections. It was thought that, in addition to providing data for the design of these larger tunnels, a quarter-scale model would itself be useful for tests on aerofoils and for other experiments.

2. *Description of Wind Tunnel.*—The 9 × 3 in. tunnel is driven from the existing compressed-air storage receivers and compressors through a 3-in. diameter pipe. This pipe together with the pressure chamber of the tunnel is designed to withstand the full available pressure of 25 atmospheres. The general arrangement is shown in Figs. 1 and 2 and details of the design are outlined in the following sections. Data relating to the design are set out in Table 1. As in the other N.P.L. tunnels, drying of the air in the tunnel depends on the displacement of moist air by the dry air injected to drive the tunnel.

The pressure chamber and the working-section were designed so that the tunnel could be converted to be 6 in. wide with the minimum of alteration to the metal work. Thus, the casting of the pressure chamber is large enough to house a 6-in. wide injector, and the width of the working-section could be doubled by doubling the widths of the top and bottom channels. A new wooden contraction and wooden first diffuser would be needed if it were decided to widen the tunnel, and the contraction ratio and the area ratio at the first corner would, of course, be halved. These precautions were taken since it was felt that a 3 in. tunnel might be too narrow for some experiments. It is not proposed to reproduce the arrangement on the 36 × 12 in. tunnels.

* Published with the permission of the Director, National Physical Laboratory.

† After this report was written it was decided to build one of the new tunnels with a working-section 36 × 14 in., and the other with a working-section 25 × 20 in.

TABLE 1

Details of 9 × 3 in. Wind-Tunnel

(Note: All area ratios are based on a nominal 9 × 3 in. working-section.)

Injector (*see* Fig. 3)	
Dimensions of tunnel at injector	9·75 × 3·0 in. (25 × 7½ cm)
Minimum width of injector slot	0·003 in. (0·08 mm)
Maximum width of injector slot	0·119 in. (3 mm)
Minimum area ratio of injector slot	0·0028
Maximum area ratio of injector slot	0·1125
Maximum total head of inducing air	25 atm
Total temperature of inducing air	roughly atmospheric
Working-Section (*see* Fig. 4)	
Maximum length	nominally 36 in. (91½ cm)
Maximum height	9·75 in. (25 cm)
Width	3·0 in. (7½ cm)
Total head of induced air	roughly atmospheric
Total dry-bulb temperature of induced air	roughly atmospheric
Relative humidity of air upstream of contraction*	roughly 10 per cent
Contraction	
Contraction ratio	16 : 1
Dimensions upstream of contraction	21 × 21 in. (53 × 53 cm)
Gauze Screens	
Upstream of contraction	up to 4 screens
Downstream of exit valve	1 screen
Downstream of first diffuser section	stop net
Corner Vanes	
Thickness (uniform)	0·036 in. (0·9 mm)
Chord	2·75 in. (7 cm)
Gap/chord ratio	0·25
First Diffuser Section	
Whole angle between top and bottom walls†	4 deg
Whole angle between side walls	6·5 deg
Area ratio at first corner	6·5 : 1
Dimensions at first corner	15·2 × 11·5 in. (38½ × 29 cm)
Second Diffuser Section	
Whole angle between top and bottom walls	3·7 deg
Whole angle between side walls	7·6 deg
Area ratio at second corner	8·3 : 1
Dimensions at second corner	16·3 × 13·75 in. (41½ × 35 cm)

* Depending on the pressure in the storage reservoir. This figure will be reduced to about 1 per cent when a new plant for drying the compressed air has been installed.

† The 9 in. dimensions of the working-section are in a vertical plane and will be referred to as the sides, the horizontal 3 in. dimensions will be referred to as the top and bottom.

Third Diffuser Section

Whole angle between top and bottom walls	0·95 deg
Whole angle between side walls	2·1 deg
Area ratio at third corner	16 : 1
Dimensions at third corner	21 × 21 in. (53 × 53 cm)

Fourth Diffuser Section

Whole angle between top and bottom walls	0 deg
Whole angle between side walls	0 deg
Area ratio at fourth corner	16 : 1
Dimensions at fourth corner	21 × 21 in. (53 × 53 cm)

Exit valve (*see* Fig. 5)

Minimum width of exit slot	0
Maximum width of exit slot	1·5 in. (3·8 cm)
Dimensions at exit slot	$18\frac{1}{2} \times 18\frac{1}{2}$ in. (47 × 47 cm)
Minimum area ratio of exit slot	0
Maximum area ratio of exit slot	4 : 1

Note: The cross-section of the tunnel increases suddenly at the exit slot from $18\frac{1}{2} \times 18\frac{1}{2}$ in. to 21 × 21 in. (*see* Fig. 5).

Safety Valves

Total area when fully open	roughly 90 sq in.
Maximum pressure excess of total head of induced air	0·05 atm

2.1. *The Injector and Pressure Chamber.*—In order that an induced-flow tunnel supplied from compressed-air storage shall operate as efficiently as possible over a range of Mach number it is desirable[3] that the area of the injector slot shall be adjustable. If Mach numbers in excess of those obtained in the present experiments (1·8) are required, it may be necessary to use an injector slot of convergent-divergent shape instead of the wholly convergent shape used in the present tunnel. It was, therefore, desirable to construct the injector so that the slot widths could be varied, and so that a convergent-divergent slot of adjustable area ratio could, if necessary, be constructed without serious difficulty. This has been done by forming the slot between two detachable pieces (A and B of Fig. 3) termed the nozzle and antinozzle, the former being fixed and the latter adjustable. In the present tunnel these are shaped to a wholly convergent slot of adjustable width giving critical sonic conditions at exit followed, under most working conditions, by an expansion of the inducing air as a partially free supersonic jet. They could, however, be replaced by new pieces to give a nozzle-shaped slot whose area ratio could be varied by moving the antinozzle.

The pressure chamber containing the injector is located immediately downstream of the working-section as shown in Fig. 2; details of its construction are shown in Fig. 3. The compressed air enters a ring-main surrounding the tunnel through four entries I supplied by a symmetrical system of pipe work. It then passes into the tunnel through four separate injector slots one in each wall of the tunnel. Each antinozzle piece B and B′ is connected by rods C to a piston P (two pistons in the case of B′) of the same area so that the pressure on the inner face of the antinozzle piece is balanced*. The pistons with their attached antinozzles may be moved along cylinders by screws driven by worms operated by the hand-wheels H,

* The sub-atmospheric pressure in the tunnel on the outer face of the antinozzle remains unbalanced, but the mechanical advantage of the system is sufficient for there to be no detectable change in the torque required to rotate the hand-wheels H when the pressure is applied. In the new 18 × 14 in. tunnel[4], which is to work with the total head of the induced air up to 3 atm absolute, complete pressure balance is accomplished by drilling the tie-rods C so that the pressure in the tunnel is equal to that on the outer face of the pistons.

thus altering the width of the injector slots. The seals between the cylinders and pistons are made by means of piston rings, and the whole assembly has been found to be remarkably free from leaks. The widths of the slots are indicated directly by Veeder counters attached to the hand-wheels H and reading in thousandths of an inch.

One practical disadvantage of the arrangement has been found to be that dirt which is present in the inducing air may become lodged in the slot and lead to mechanical damage if the slot is then closed. This has been overcome by placing an improved air filter in the supply system, an earlier filter having failed and led to damage of the type described.

2.2. *The Exit Valve.*—In order to keep the pressure in the tunnel constant, a quantity of air equal to that which is injected through the injector slot is allowed to escape through the exit valve. This valve is located immediately upstream of the third corner (*see* Fig. 2) and is shown in detail in Fig. 5. In principle it is essentially a backward-facing suction slot at which a small amount of diffusion is allowed to occur suddenly. Referring to Fig. 5, the slot is formed between a fixed piece D and the end of a flexible metal plate A which is built-in at the downstream end and supported at the upstream end by rods C attached to a stiffening rib soldered to plate A. The width of the slot is adjusted by flexing the plate by withdrawing the rods C with a rack and pinion E. The rods C of all four exit slots are connected to a hand-lever by a single continuous chain F. The air which is withdrawn passes into an annular chamber which surrounds the tunnel, and thence into a duct which removes it from the tunnel room.

2.3. *The Working-Section.*—The top and bottom members of the working-section (*see* Fig. 4) are cast-iron channels 3 in. wide. These are drilled to take the bolts which hold the wooden liners, and to allow the pressure-measuring tubes to be brought out of the tunnel. A pair of adjustable walls made of flexible steel plate are being constructed for the tunnel. These are to be shaped by micrometer screws passing out through the top and bottom channels in a manner similar to that used on the 20 $\times$ 8 in. tunnel.

The sides of the working-section are formed by brass plates fitted with 1-in. thick glass suitable for schlieren work. The lengths of these plates are so arranged that the turntables in which the model is held may be placed within 4 in. of any point along the length of the working-section. The seals between the side plates, and between these plates and the top and bottom channels are accomplished entirely by metal-to-metal butt joints, the faces of the individual plates being made true to within 0·0004 in. This has been done to ensure that the interior surface of the working-section is free from steps or gaps.

The model is held between turntables fitted with 13-in. diameter glass windows and its incidence is adjusted by rotating the turntables which are interconnected by a shaft passing through a clearance hole in one of the wooden liners of the working section.

The 9-in. sides of the working-section are parallel and all allowance for the growth of the boundary layers on the walls is made on the 3-in. wooden liners at the top and bottom. Wooden liners are available for subsonic running and for supersonic work at Mach numbers of 1·4, 1·6 and 1·8. Delay in the manufacture of the exploring apparatus for the working-section has prevented a detailed examination of the flow here, but schlieren observations have shown the supersonic liners to give streams which appear to be substantially free from wavelets. The shapes of the liners are set out in Table 2 and shown in Fig. 6. This diagram also shows the positions of the regions of constant Mach number (' test diamonds ') for the supersonic liners.

The pressure distributions along the subsonic liners are shown in Fig. 7, and it is clear that the allowance which was made for the growth of the boundary layer (0·009 in. per in. on each of the two liners) is rather too large. This allowance was calculated from Refs. 5, 6 and R. & M. 2068[7] on the assumption that the boundary layer was turbulent. It is proposed to modify the liners in an attempt to obtain a more uniform pressure distribution.

TABLE 2

Shapes of Supersonic Liners

$M = 1{\cdot}4$		$M = 1{\cdot}6$				$M = 1{\cdot}8$			
x	y	x	y	x	y	x	y	x	y
0	0·558	0	0·558	22·373	1·957	0	0·558	17·939	3·139
0·05	0·586	0·3	0·727	22·813	1·953	0·5	0·83	18·260	3·134
0·169	0·672	0·6	0·894	23·254	1·948	1·0	1·15	18·590	3·130
0·684	0·927	0·64	0·90	23·695	1·944	1·5	1·46	18·921	3·126
1·160	1·170	0·79	0·981	24·0	1·938	2·0	1·77	19·251	3·123
1·636	1·387	1·24	1·223	24·5	1·933	2·9	2·360	19·5	3·120
2·112	1·554	1·69	1·464	25·0	1·926	3·285	2·566	20·0	3·115
2·588	1·690	2·14	1·698	25·5	1·920	3·615	2·745	20·5	3·110
3·063	1·774	2·59	1·889	26·0	1·915	3·945	2·922	21·0	3·103
3·539	1·910	3·04	2·050	26·5	1·907	4·205	3·099	21·5	3·087
4·015	2·002	3·49	2·199	27·0	1·897	4·605	3·270	22·0	3·054
4·491	2·083	3·94	2·334	27·5	1·886	4·935	3·430	Straight	
4·967	2·150	4·39	2·455	Straight		5·265	3·560	44·0	1·5
5·442	2·205	4·84	2·565	44·0	1·5	5·595	3·671		
5·918	2·248	5·29	2·661			5·925	3·771		
6·394	2·280	5·74	2·742			6·255	3·860		
6·870	2·297	6·19	2·811			6·585	3·939		
7·346	2·304	6·64	2·866			6·915	4·007		
7·821	2·294	7·09	2·908			7·245	4·065		
8·297	2·274	7·54	2·938			7·575	4·112		
8·773	2·247	7·99	2·953			7·905	4·149		
9·250	2·215	8·29	2·956			8·235	4·171		
9·725	2·179	8·708	2·949			8·565	4·191		
10·200	2·142	9·149	2·926			8·895	4·197		
10·676	2·104	9·590	2·893			9·115	4·186		
11·152	2·068	10·031	2·850			9·336	4·161		
11·628	2·031	10·472	2·799			9·556	4·126		
12·104	1·996	10·912	2·743			9·776	4·085		
12·579	1·963	11·353	2·685			9·997	4·043		
13·055	1·931	11·794	2·626			10·217	4·00		
13·531	1·903	12·235	2·568			10·437	3·958		
14·007	1·876	12·676	2·512			10·658	3·915		
14·483	1·852	13·117	2·458			10·988	3·851		
14·958	1·830	13·556	2·407			11·319	3·790		
15·434	1·811	13·997	2·359			11·649	3·729		
15·914	1·793	14·438	2·314			11·980	3·671		
16·386	1·779	14·879	2·272			12·310	3·616		
16·862	1·765	15·320	2·232			12·642	3·562		
17·337	1·753	15·761	2·194			12·972	3·512		
17·813	1·744	16·202	2·163			13·302	3·465		
18·289	1·736	16·642	2·131			13·633	3·421		
18·765	1·730	17·083	2·106			13·964	3·381		
19·241	1·723	17·524	2·080			14·294	3·345		
19·716	1·719	17·965	2·056			14·625	3·312		
20·192	1·714	18·406	2·038			14·955	3·282		
20·668	1·709	18·847	2·022			15·286	3·267		
21·144	1·704	19·288	2·008			15·616	3·233		
21·620	1·701	19·727	1·998			15·947	3·212		
Straight		20·168	1·989			16·277	3·193		
44·0	1·500	20·609	1·981			16·608	3·178		
		21·050	1·974			16·938	3·165		
		21·491	1·969			17·268	3·154		
		21·932	1·963			17·599	3·146		

With an injector of the type used, the Mach number which can be reached in the working-section is limited (R. & M. 2448[8]) by choking caused by the formation of a throat in the tunnel by the inducing air before mixing takes place. Choking can be postponed, and a higher Mach number attained, by reducing the size of the working-section by placing an expanding channel between it and the injector. Following some preliminary experiments in a 2-in. square tunnel, the liner shown in Fig. 6 was designed for the 9 × 3 in. tunnel and a Mach number of 1·8 reached. Mach numbers up to 2·0 were obtained in the 2-in. tunnel, but the working-section of the 9 × 3 in. tunnel was too short to enable the required shape to be reproduced. An attempt to obtain a Mach number of 2·0 in the 9 × 3 in. tunnel by making the expansion upstream of the injector with an angle of 12 deg between the top and bottom walls* was a failure, the flow separating from the walls and the tunnel shock-wave remaining in the nozzle. It was found that under these conditions the injector could maintain the greatest pressure ratio at the widest injector slot width, that is, the tunnel shock-wave could be forced further downstream at wide than at narrow slot widths. It is thought that the efficiency could be improved and higher Mach numbers obtained by improving the efficiency of diffusion between the working-section and injector. This would require that some form of supersonic diffuser (other than a near-normal shock wave) should be inserted ahead of the expanding channel. If this were to be done, however, the working-section would need to be lengthened. This might also be desirable if a choked throat[9, 10, 11] is to be used at the downstream end of the subsonic working-section to prevent disturbances from the injector passing upstream†. A longer working-section would also facilitate the design of liners containing slotted walls for the reduction of tunnel interference at transonic speeds.

Since it is known[12] that the length of the working-section has little effect upon the power requirements, it is suggested that the present length of the working-sections of the proposed 36 × 12 in. wind tunnels should be increased by about 6 ft, a similar length being added between the second and third corners to complete the circuit.

2.4. *The Return Circuit.*—The return circuit is constructed in the main of $\frac{5}{8}$ in. plywood and is of rectangular section throughout. The corners are fitted with cascades of 0·036-in. sheet metal vanes of the type recommended by Salter (R. & M. 2469[13]), the gap/chord ratio is 0·25. Each corner is fitted with glass panels in the side walls to enable the flow to be visualized by streamers. Safety valves designed to limit the pressure in the tunnel to 1·05 atm are fitted in the wall of the long arm of the return circuit. Bushes for the insertion of exploring apparatus are provided at several points round the tunnel circuit as shown in Fig. 2.

2.5. *The Contraction.*—The contraction was designed on the basis of a method described by Cheers (R. & M. 2137[14]) and has a ratio of 16 : 1. The method consisted simply of designing two of Cheers' curves, one leading up to the long and the other to the short side of the working-section, the longer sides becoming parallel roughly 10 in. further upstream than the shorter (the distance depending upon the liners which are being used in the working section). This application of Cheers' method has little theoretical justification, but unpublished pressure measurements‡ indicated that over a wide range of working-section Mach number it gave a channel along which the pressure fell monotonically.

2.6. *Gauze Screens.*—Provision was made for the insertion of a stop-net at the downstream end of the first diffuser section to protect the corner vanes in the event of a model becoming loose in the working-section. A frame in which a gauze damping screen could be placed was provided downstream of the exit valve and four similar frames were located upstream of the contraction. The positions of the screens are shown in Fig. 2. Details of the gauzes used are given in Table 3.

* The corresponding angle in the 2-in. tunnel was 6 deg.

† The observations reported in section 4 suggest that noise from the injector forms a major part of the turbulence in the working-section at low speeds.

‡ Made by A. E. Knowler.

TABLE 3

Details of Gauzes Used

Mesh per inch	Wire diameter in.	Reynolds number of wireat 40 ft/sec	Pressure-drop coefficient
4	0·048	Stop Net	
30	0·01	210	2·0
100	0·0044	90	7·0

The pressure-drop coefficient is defined as the difference between the static pressures upstream and downstream of the gauze divided by the dynamic head. The coefficients tabulated have been taken from R. & M. 2276[15], these values being in good agreement with those observed in the present experiment. The speed of 40 ft/sec used in defining the Reynolds number of the wires is the mean speed downstream of the exit valve and upstream of the contraction when the working-section Mach number is 0·9. The 30-mesh gauze was chosen to have a pressure-drop coefficient of 2 to satisfy the criterion given by Collar (R. & M. 1867[16]) and by Batchelor[17] for the removal of spatial non-uniformity. The 100-mesh gauze was selected for a high pressure-drop coefficient in order to reduce the turbulence[18], and the small wire diameter was chosen to reduce the turbulence introduced by the screen itself.

3. *Flow in the Tunnel Circuit.*—The distributions of pitot and static pressure were measured at eight stations round the circuit along two perpendicular lines parallel to the walls of the tunnel and passing through the axis. The measurements were made at a working-section Mach number of 0·9 and at injector slot widths of 0·02 and 0·119 in. Separate pitot and static tubes each of external diameter 0·05 were used in turn, the datum pressure (H_0) being the total head measured at a fixed pitot-tube immediately upstream of the contraction. Pressure differences were measured with a 26 in. Chattock gauge or with an alcohol tube inclined at 5 deg or at 10 deg to the horizontal; a vertical mercury tube was used for some of the measurements immediately downstream of the injector slot.

The static pressure at each station was found to be constant across the tunnel to within 0·005 in. of water. Since the unsteady fluctuations of the tunnel were of this order and there was a considerable lag in the manometer, accurate measurements were not possible, and a mean value of the static pressure across the tunnel has been used in calculating the velocities. The uniformity of the static pressure shows that the flow is sensibly free from swirl.

The velocity profiles observed with the tunnel in its original condition are shown in Fig. 8. The velocity peaks associated with the high-velocity air stream injected through the 3-in. long injector slots have disappeared at the second corner, but those associated with the air injected through the 9-in. slots persist at the beginning of the long arm of the return circuit. At both slot widths the velocity profiles just upstream of the exit valve are, however, free from peaks associated with the injected air, but are asymmetrical, the velocity being high towards the inside of the circuit. Since no serious overturning could be detected at the second corner, this asymmetry seems to be accentuated in the diffuser between the second corner and the exit valve. The asymmetry upstream of the exit valve is more pronounced with the wide than with the narrow injector slot width. The variations of total head across the tunnel upstream and downstream of the exit valve are shown in Figs. 9, 10 and 11. These show that at the narrow injector slot width the distribution across the tunnel does not change greatly after passing the exit slot and is moreover not sensitive to the exit slot width. At the wide injector slot width, however, the asymmetry is increased on passing the exit slot and a separation occurs from the lip of the slot on the outside of the circuit. The distribution downstream is more sensitive to the width of the exit slot than for the narrower injector slot.

By the time the flow has reached the upstream end of the contraction, however, the velocity profiles for the two injector slot widths are virtually identical and both show a marked asymmetry with a region of high velocity close to the inside of the circuit. The flow is more uniform across the tunnel in a direction parallel to the 9-in. dimension of the working-section. The distributions upstream of the contraction were independent of the width of the exit slot.

It was found that the distribution ahead of the contraction could be greatly improved by inserting a gauze screen of pressure-drop coefficient 2·0 downstream of the exit valve. The effect of this screen and of other screen combinations on the flow ahead of the contraction is shown in Figs. 12 and 13. The gauze arrangements used are set out in Table 4.

TABLE 4

Gauze Arrangements Used

Gauze arrangement number	Mesh per inch of screen at gauze position (Fig. 2)					
	A	B	C	D	E	F
1	4	—	—	—	—	—
2	4	30	—	—	—	—
3	4	30	30	—	—	—
4	4	30	30	100	100	100
5	4	30	—	100	—	—
6	4	30	—	100	100	—
7	4	30	—	100	100	100
8	—	30	—	—	—	—
9	—	—	30	100	100	100
10	—	30	30	100	100	100

The empty-tunnel distribution was slightly improved by the insertion of the stop-net upstream of the first corner (AA in Fig. 2). The distribution with the stop-net and exit-valve screen present was greatly improved by the insertion of a second 30-mesh screen ahead of the contraction. The addition of 100-mesh screens of pressure-drop coefficient 7·0 downstream of this screen has an adverse effect on the total-head distribution, and this is probably due to the fact that they were not quite uniform. These high-resistance screens had, however, a favourable effect on the turbulence (*see* section 4).

The simple theory put forward by Collar (R. & M. 1866[19]) suggests that the ratio of a spatial velocity perturbation to the mean velocity across the tunnel will be reduced on contraction by the square of the contraction ratio. The effect of compressibility on this reduction factor will be to increase it by roughly the square of the ratio of the densities upstream and downstream of the contraction. Thus since the velocity distribution ahead of the contraction is uniform, that at the entry to the working-section would be expected to be very good.

Static-pressure measurements along the walls of the first diffuser between the injector and the first corner are shown in Fig. 14. These show that the static pressure rises continuously along the diffuser and, together with the measurements across the tunnel upstream of the first corner, suggest that the flow is not separating from the walls.

4. *Turbulence Measurements.*—The root-mean-square values (u') of the longitudinal component of the turbulent velocity fluctuations were measured with a hot-wire upstream of the contraction and in the working-section (*see* Fig. 15). The measurements in the working-section were made at low speeds only (up to 200 ft/sec). No measurements of the transverse components of the turbulent fluctuations were made. The stop-net and a single 30-mesh screen downstream of the exit valve were present throughout the measurements. The results are set out in Tables 5 and 6.

4.1. *Turbulence Upstream of the Contraction.*—The intensity of the longitudinal component of the turbulence (u'/U) based on the speed upstream of the contraction is plotted as a function of working-section Mach number in Fig. 16. The turbulence increases in a manner which is very roughly proportional to the Mach number and does not depend greatly on the injector

TABLE 5

Turbulence Upstream of Contraction

Working-section		Slot width (in.)	Screen mesh per inch*				Based on velocity upstream of contraction
Mach Number	Velocity (ft/sec)		C	D	E	F	u'/U (per cent)
0·7		0·02	—	—	—	—	1·62
0·9		0·02	—	—	—	—	1·94
0·9		0·119	—	—	—	—	1·91
1·6		0·02	—	—	—	—	4·19
1·6		0·119	—	—	—	—	3·22
0·11	120	0·02	—	—	—	—	0·74
0·7		0·02	30	—	—	—	0·80
0·9		0·02	30	—	—	—	0·89
0·9		0·119	30	—	—	—	0·85
0·9		0·02	100	—	—	—	0·89
0·9		0·02	30	—	—	100	0·71
0·9		0·02	30	100	—	—	0·75
0·9		0·02	100	—	—	30	0·73
0·7		0·02	30	100	100	100	0·47
0·9		0·02	30	100	100	100	0·47
0·9		0·119	30	100	100	100	0·47
1·6		0·02	30	100	100	100	0·89
1·6		0·119	30	100	100	100	0·93
0·11	120	0·02	30	100	100	100	0·04

* The screen letters refer to Figs. 2 and 15.

slot width. Table 5 shows that the turbulence is lowest when all four screens are present (the pressure-drop coefficients are given in Table 3) being a little less than $\frac{1}{2}$ per cent at top subsonic speed and nearly double this at a Mach number of 1·6. For single screens the quantity u'/U is plotted against the pressure-drop coefficient (k) in Fig. 17. It appears that the reduction of turbulence produced by increasing the pressure-drop coefficient beyond 2·0 is comparatively small.

The limited set of observations which were made are in fair agreement (Fig. 17) with the predictions of Dryden and Schubauer[18]. For a number of widely spaced screens in sequence with individual pressure-drop coefficients k_1, k_2, k_3 . . . Dryden and Schubauer suggest that the reduction of turbulence is given by $1/\sqrt{(1 + k_1)}\sqrt{(1 + k_2)}\sqrt{(1 + k_3)}$ . . . . The observed turbulence with four screens in position is plotted in Fig. 17 at a pressure-drop coefficient equal to the sum of the individual coefficients of the screens and is seen to be in fair agreement with the curve $1/\sqrt{(1 + \Sigma k)}$. The value corresponding to $1/\sqrt{(1 + k_1)}\sqrt{(1 + k_2)}\sqrt{(1 + k_3)}$ . . . is considerably lower than the observed value. Table 5 shows that the turbulence downstream is roughly the same for a 30-mesh screen followed by a 100-mesh screen as for a 100-mesh followed by a 30-mesh screen. Provided that the turbulence introduced by the screen is allowed to decay this observation is again in accordance with Dryden and Schubauer's suggestion that the pressure-drop coefficient is the important parameter. The use of a fine screen upstream of one with a pressure-drop coefficient of about two has certain advantages* since the coarse screen is thus protected from dust and oil, and moreover, gives a good velocity distribution downstream. Table 5 also suggests that within the limits used the spacing of the screens has a relatively small effect upon the turbulence.

4.2. *Turbulence in the Working-Section.*—Table 6 shows that at low speeds the turbulence in the working-section depends considerably on the slot width. The lowest value of u'/U which was measured is 0·09 per cent which is double that upstream of the contraction. Since u'/U might be expected (R. & M.'s 1866[19], 2437[21] and Refs. 22, 23) to decrease on contraction, and since there is an effect of varying slot width†, it is thought that noise from the injector plays an important part in determining the turbulence in the working-section. It has been known for some time that induced-flow tunnels of the type used become more noisy as the slot width is increased.

TABLE 6

Turbulence in Working-Section

Velocity in working-section (ft/sec)	Slot width (in.)	Screen mesh per inch‡				Based on velocity in working-section u'/U per cent
		C	D	E	F	
120	0·02	—	—	—	—	0·21
120	0·119	—	—	—	—	0·35
120	0·02	30	100	100	100	0·09
120	0·119	30	100	100	100	0·34
200	0·02	30	100	100	100	0·29
200	0·119	30	100	100	100	0·39

‡ The screen letters refer to Figs. 2 and 15.

* This arrangement has been used for some years on the 20 × 8 in. wind tunnel at the N.P.L. In this case, however, the fine screen is in a region of larger cross-sectional area and lower velocity than the coarse screen.

† Being absent ahead of the contraction this effect is presumably caused by noise passing upstream into the working-section.

It is not known how much the contribution of noise to the turbulence in the working-section varies with Mach number. Photographs taken with a sensitive schlieren apparatus and an exposure of less than one microsecond have not, however, revealed any intense moving waves of the type reported in Refs. 9 and 10 in the empty working-section up to the top subsonic speed. Nevertheless it seems desirable to make provision for adjustable throats at the downstream ends of the working-sections of the 36 × 12 in. wind tunnels so that small regions of supersonic flow may be interposed between the injectors and working-sections.

The effects of noise from downstream are, of course, absent when the tunnel is working with a supersonic speed in the working-section.

4.3. *Comparison with Other Tunnels.*—Since the data on the effect of contraction on the turbulence of a stream are inconsistent at low speeds and the effects of compressibility are unknown, it is not possible to estimate the turbulence in the working-section of the present tunnel at high Mach number from the observations upstream of the contraction. If, however, the value of u'/U in the empty tunnel upstream of the contraction may be taken as a measure of the general level of the turbulence Table 7 shows that the 9 × 3 in. wind tunnel compares favourably with the few low-speed tunnels for which data are available.

TABLE 7

Turbulence Upstream of the Contractions of Several Wind Tunnels

Wind tunnel	u'/U per cent	Speed in working-section
N.P.L. Low Turbulence*	3	Low Speed
Cambridge (R. & M. 1842[20])	3·5	
N.B.S. 4½ ft (Ref. 18)	2·3	
9 × 3 in.	0·7	
9 × 3 in.	1·9	$M = 0{\cdot}9$
9 × 3 in.	3·5	$M = 1{\cdot}6$

* From some unpublished work by L. F. G. Simmons and R. W. Gould.

5. *Power Requirements.*—The variation of the total head of the inducing air (termed the blowing pressure) with the width of the injector slot and the Mach number is shown in Fig. 18. Corresponding values of the mass ratio (the ratio of the rate of mass flow of induced to that of inducing air) are shown in Fig. 19. They have been calculated from the measured blowing pressures on the assumption that the injector slot is choked*. The area ratios of the abscissae of Figs. 18 and 19 are based on a nominal working-section area of 27 sq in.

Comparison of Fig. 18 with the observations reported in Ref. 3 shows that except for very narrow slot widths the blowing pressures of the 9 × 3 in. wind tunnel are rather greater than those required for the 2¼-in. diameter tunnel. This is attributed mainly to the change in the cross-sectional shape in the vicinity of the injector. An earlier investigation[24] which suggested that the cross-sectional shape had little effect on the blowing pressure did not include a shape as extreme as a 3 : 1 rectangle. The discrepancies are however not sufficient to invalidate general performance predictions based on the measurements made in the 2¼-in. tunnel (*e.g.*, in Ref. 3).

The influence of the stop-net and gauze screens on the blowing pressure is shown in Table 8.

* The curves are shown dotted at blowing pressures below that at which the injector slot becomes choked.

TABLE 8

Influence of Gauze Screens on the Blowing Pressure

$M = 0{\cdot}9$

Gauze arrangement*	P/H at slot width (in.)			
	0·119	0·060	0·020	0·003
Empty Tunnel	2·35	3·50	7·16	16·30
No. 8	2·35	3·50	7·16	16·30
No. 1	2·42	3·61	7·56	16·86
No. 9	2·50	3·72	7·71	17·60
No. 10	2·55	3·78	7·96	18·10
No. 4	2·62	4·05	8·32	18·97

* *See* Table 4.

It is proposed to install compressed-air receivers with a total volume of 12,500 cu ft at the West Aero. site at the N.P.L. If the tunnel is started when the pressure in these is the maximum value of 25 atm absolute then the possible maximum durations of tunnel runs on each of the 3×1 ft wind tunnels will be of the order shown in Table 9. These values have been calculated from the measurements on the 9×3 in. tunnel in the manner suggested in Ref. 3.

TABLE 9

Estimated Maximum Duration of Runs on 3×1 *ft Wind Tunnels*

Mach number in working-section	Running time, minutes
0·9	16
1·6	$3\frac{1}{2}$
1·8	$2\frac{1}{2}$

6. *Scale Effect.*—There appears to be little information on the effects of tunnel size on turbulence. It was appreciated that in order to reproduce the full-scale conditions of decay, the full-scale gauze spacing should strictly be reproduced on the model. This would, however, have given a very long settling length and would have required a departure from the scale reproduction of other parts of the circuit. The data given in Ref. 23 suggested that if the screen spacing was made to quarter-scale a considerable amount of decay would still take place between the screens and this was, therefore, done on the model, where the screen spacing was made 1·2 in. (*see* Fig. 15). From the aspect of decay between the screens and downstream in the settling length and contraction the turbulence measurements on the model may, therefore, be expected to be pessimistic. Thus since with several screens in position much of the turbulence

downstream must be introduced by the screens themselves, the measurements made under these conditions are probably pessimistic. The effect of model scale on the intensity of the turbulence in the empty tunnel and on the effects of noise is, however, less certain. A comparison[24] between observations on a $2\frac{1}{4}$-in. diameter, a 12-in. diameter and a 20 × 8 in. tunnel has suggested that there is probably little scale effect on the power requirements of induced-flow tunnels.

7. *Conclusions.*—In general the tunnel seems to be satisfactory as regards velocity distribution, turbulence and power requirements. The only major alteration to the design of the 3 × 1 ft tunnels which is suggested is that the length of the working-section shall be increased by about 6 ft.

8. *Acknowledgments.*—Mr. D. Giles and Mr. A. F. Bray were responsible for the detailed design of the tunnel. The major part was made in the Aerodynamics Division, N.P.L., Mr. R. W. Rowe being responsible for the woodwork and Mr. W. Rich and Mr. J. S. Wreford for the metalwork. The turbulence measurements were made by Mr. R. W. F. Gould, and Miss N. A. Bumstead helped throughout the experimental work and with the reduction of observations.

---

9. *List of Symbols.*

p	Local static pressure
H_0	Mean total head immediately upstream of the contraction
H	Local total head
B	Barometric pressure
A_S	Area of injector slot
A_W	Area of working-section
M	Mach number in working-section

REFERENCES

No.	Author	Title, etc.
1	A. Fage and C. H. N. Lock ..	The Proposed High-Speed Laboratory on the West Aero. Site, N.P.L. A.R.C. 9531. April, 1946. (Unpublished.)
2	J. A. Beavan and G. A. M. Hyde ..	Interim Report on the Rectangular High-Speed Tunnel Including some Pitot-Traverse Measurements of Drag of the Aerofoil E.C.1250. R. & M. 2067. February, 1942.
3	D. W. Holder	An Estimation of the Running Time of an Induction-Type High-Speed Tunnel Driven from Compressed-Air Storage. A.R.C. 9902. August, 1946. (Unpublished.)
4	Staff of the High-Speed Tunnel, N.P.L.	The New 18 × 14 in. Wind Tunnel: Position on March 31st, 1945. A.R.C. 8545. (Unpublished.)
5	W. F. Cope	The Turbulent Boundary Layer in a Compressible Flow. A.R.C. 7634. (Unpublished.)
6	W. F. Cope	The Laminar Boundary Layer in Compressible Flow. Work Performed for Ordnance Board. Communicated by Superintendent, Engineering Dept., N.P.L. A.R.C. 7635. (Unpublished.)
7	A. D. Young and N. E. Winterbottom	High-Speed Flow in Smooth Cylindrical Pipes of Circular Section. R. & M. 2068.
8	A. E. Knowler and D. W. Holder..	The Efficiency of High-Speed Wind Tunnels of the Induction Type. With an Appendix: The Efficiency of Intermittent Operation from Compressed Air Storage. R. & M. 2448. December, 1948.
9	H. Eggink	Fluctuations of Flow in High-Speed Wind Tunnels. R.A.E. Report No. Aero. 2204/S.D.18. A.R.C. 10,810. June, 1947. (Unpublished.)
10	H. Eggink	Göttingen Monograph. Model Test Technique. Test Installations. 1. On Unsteady Processes in High-Speed Tunnels. Ministry of Supply. R. & T. 948T. G.D.C. 1026T. A.R.C. 11,276. September, 1947. (Unpublished.)
11	H. W. Liepmann and H. Ashkenas	Shock-wave Oscillations in Wind Tunnels. *J. Ae. Sci.*, Vol. 14, p. 295. 1947.
12	D. W. Holder and P. M. Burrows..	Explorations Along the Axes of Two Supersonic Tunnels of the Injector Type. A.R.C. 8670. May, 1945. (Unpublished.)
13	C. Salter	Experiments on Thin Turning Vanes. R. & M. 2469. October, 1946.
14	F. Cheers	Note on Wind-Tunnel Contractions. R. & M. 2137. March, 1945.
15	L. F. G. Simmons and C. Cowdrey..	Measurement of the Aerodynamic Forces Acting on Porous Screens. R. & M. 2276. August, 1945.
16	A. R. Collar	The Effect of a Gauze on the Velocity Distribution in a Uniform Duct. R. & M. 1867. February, 1939.
17	G. K. Batchelor	On the Concept and Properties of the Idealized Hydrodynamic Resistance. A.C.A. 13. 1945.
18	Hugh L. Dryden and G. B. Schubauer	The Use of Damping Screens for the Reduction of Wind-Tunnel Turbulence. *J. Ae. Sci.*, Vol. 14, No. 4. April, 1947. A.R.C. 10,438.
19	A. R. Collar	The Use of a Windmill in a Return Flow Tunnel. R. & M. 1866. November, 1938.
20	A. A. Hall	Measurements of the Intensity and Scale of Turbulence. R. & M. 1842. August, 1938.
21	D. C. MacPhail	Turbulence Changes in Contracting and Distorted Passages. R. & M. 2437. March, 1944.
22	G. I. Taylor	Turbulence in a Contracting Stream. *Z.A.M.M.*, Vol. 15, p. 91. 1935.
23	Hugh L. Dryden	A Review of the Statistical Theory of Turbulence. From *Quarterly of Applied Mathematics*, Vol. 1, No. 1. April, 1943. A.R.C. 7208.
24	A. E. Knowler and D. W. Holder..	Scale Effect on the Efficiency of Tunnels of the Injector Type. A.R.C. 8669. May, 1945.

Refs. 3, 12 and 24 are included in ' The Efficiency of High-Speed Wind Tunnels of the Induction Type '. A.R.C. Monograph. R. & M. 2448. December, 1948.

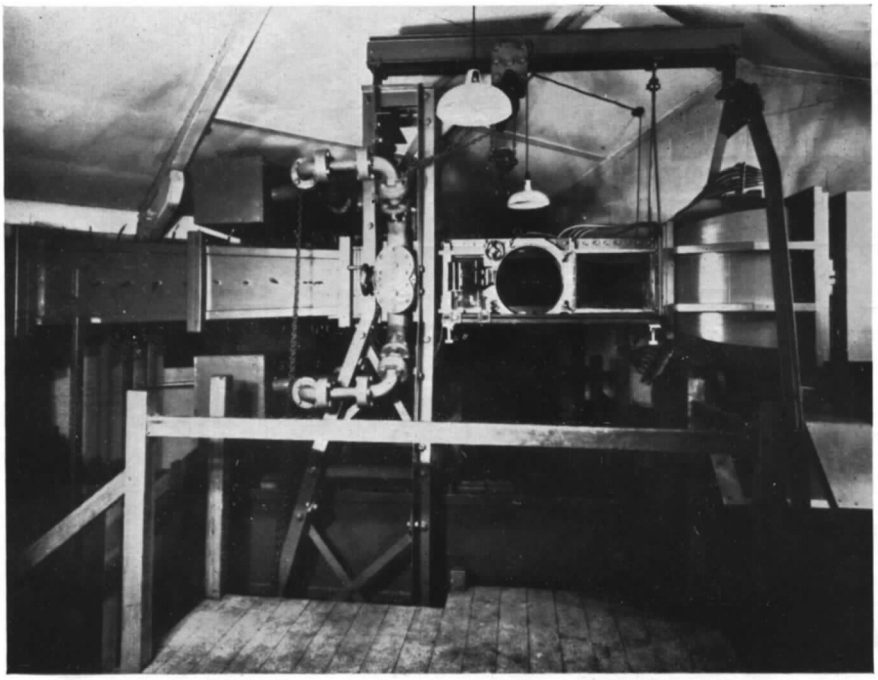

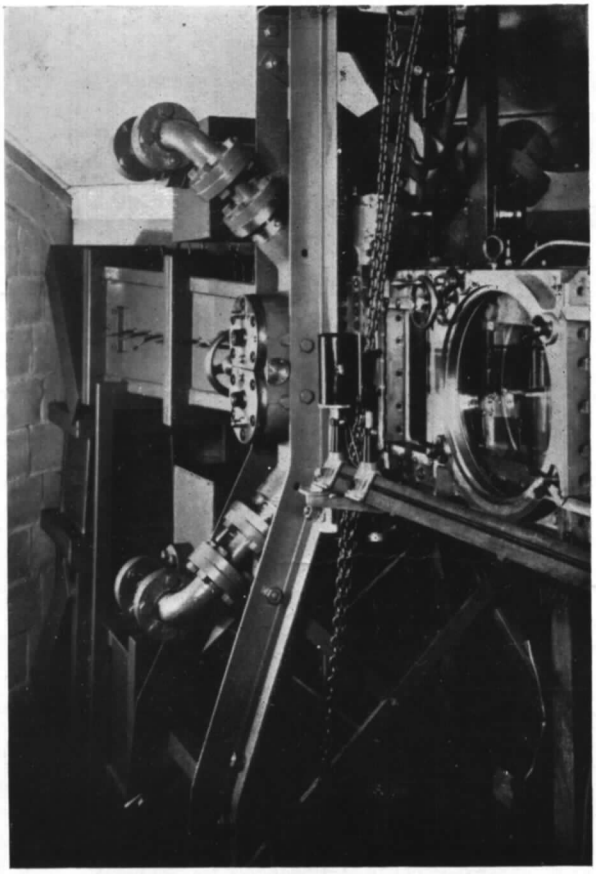

FIG. 1. Photographs of the 9×3 in. tunnel.

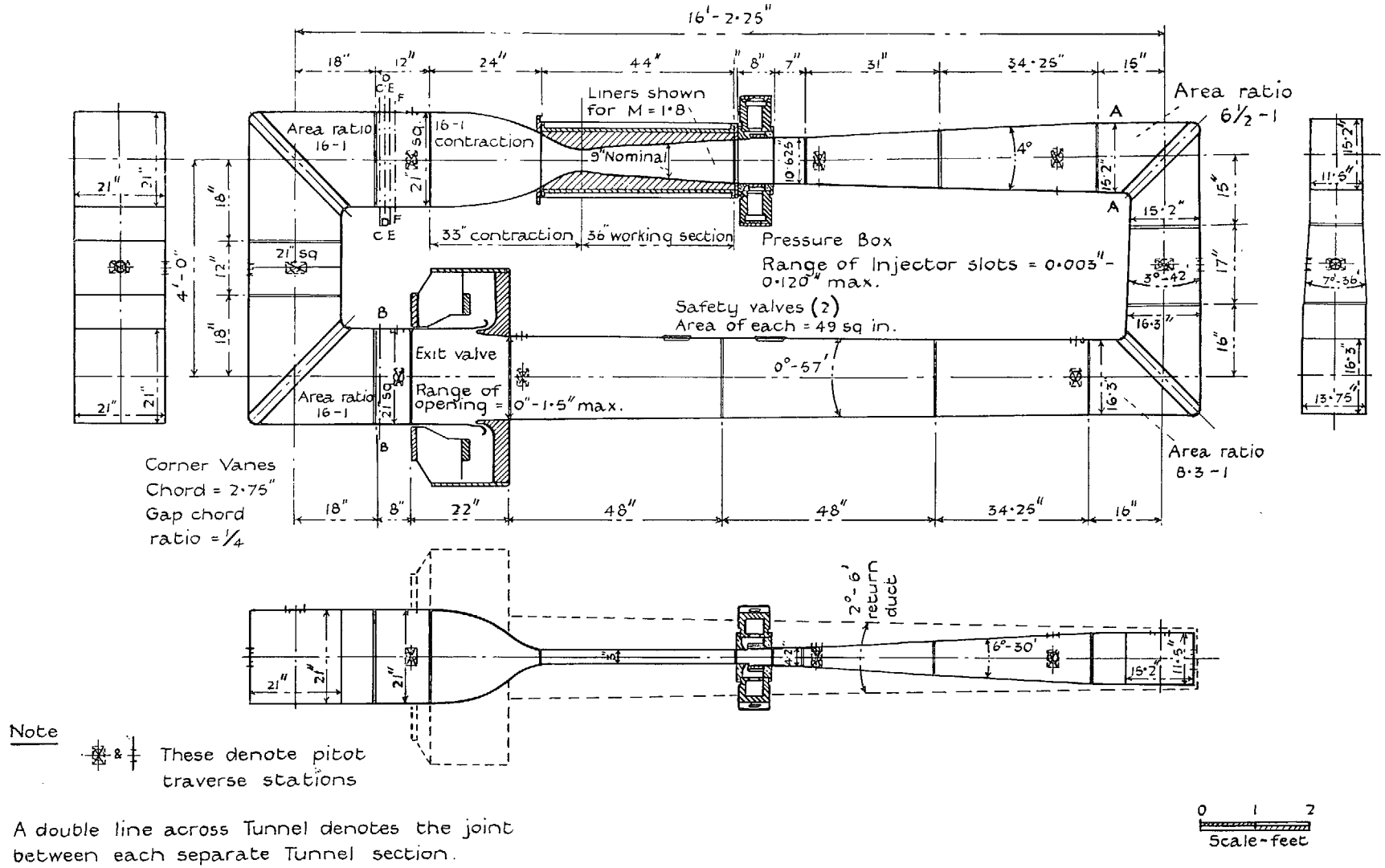

FIG. 2. 9 × 3 in. Rectangular High-Speed Tunnel. Air line of tunnel.

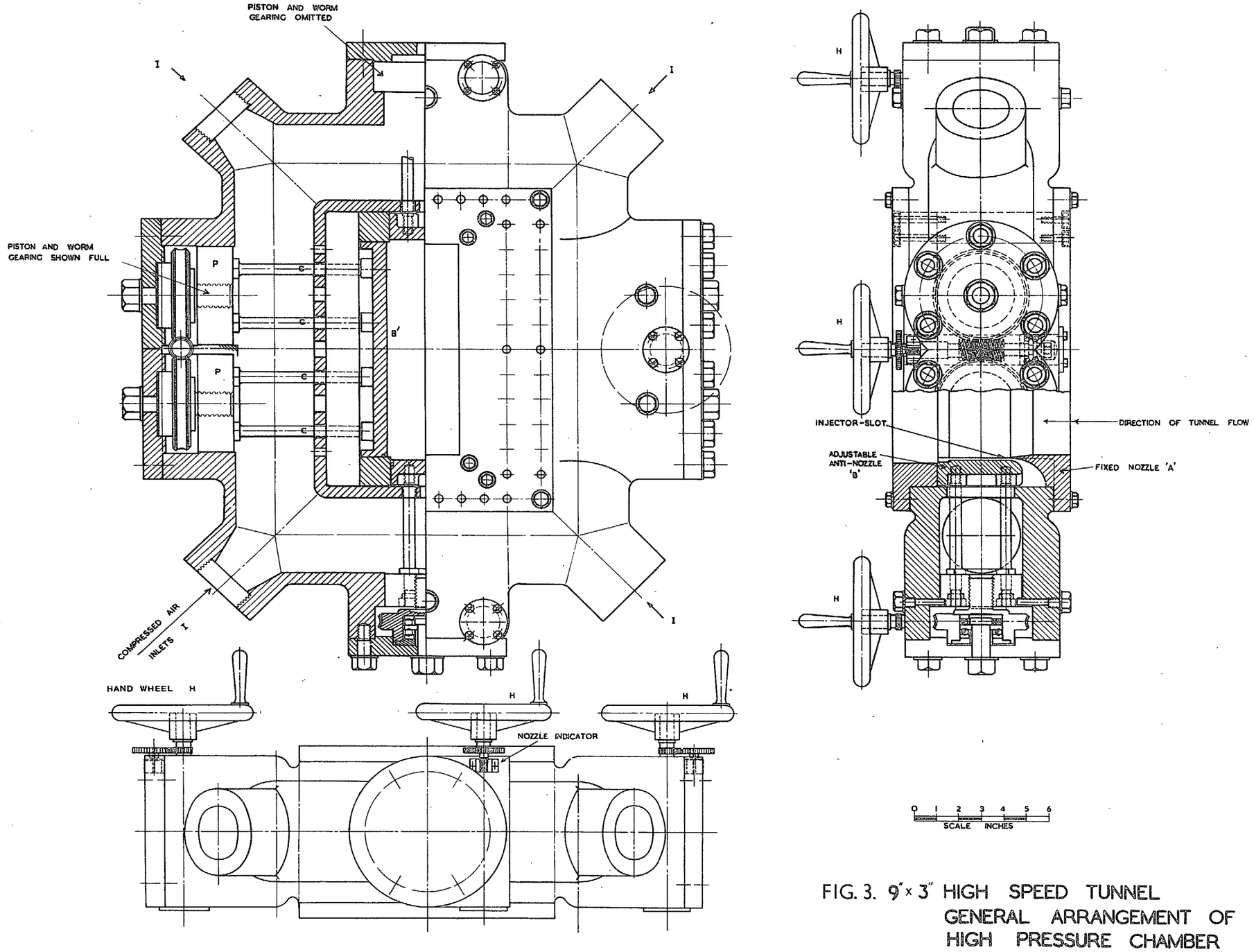

FIG. 3. 9" × 3" HIGH SPEED TUNNEL GENERAL ARRANGEMENT OF HIGH PRESSURE CHAMBER

4801-16-680-1 M-10/52. (M. F. P.)

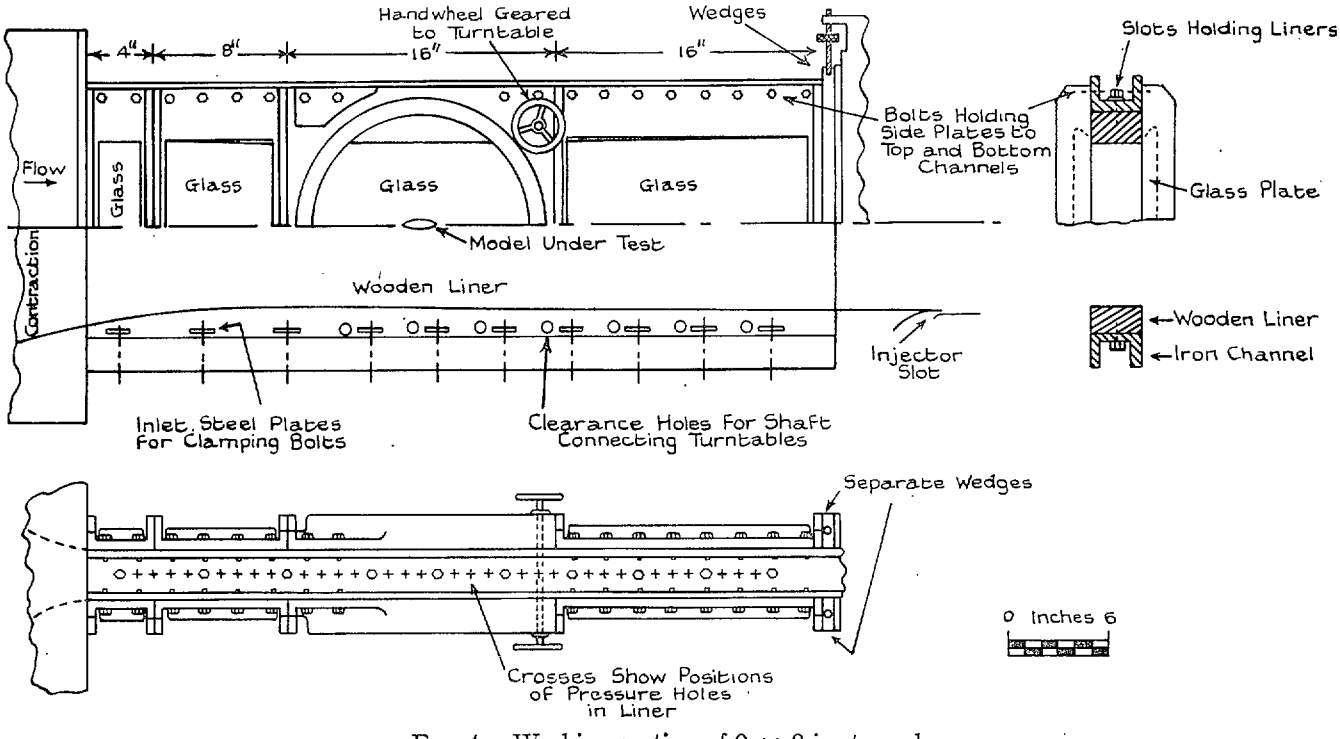

FIG. 4. Working-section of 9 × 3 in. tunnel.

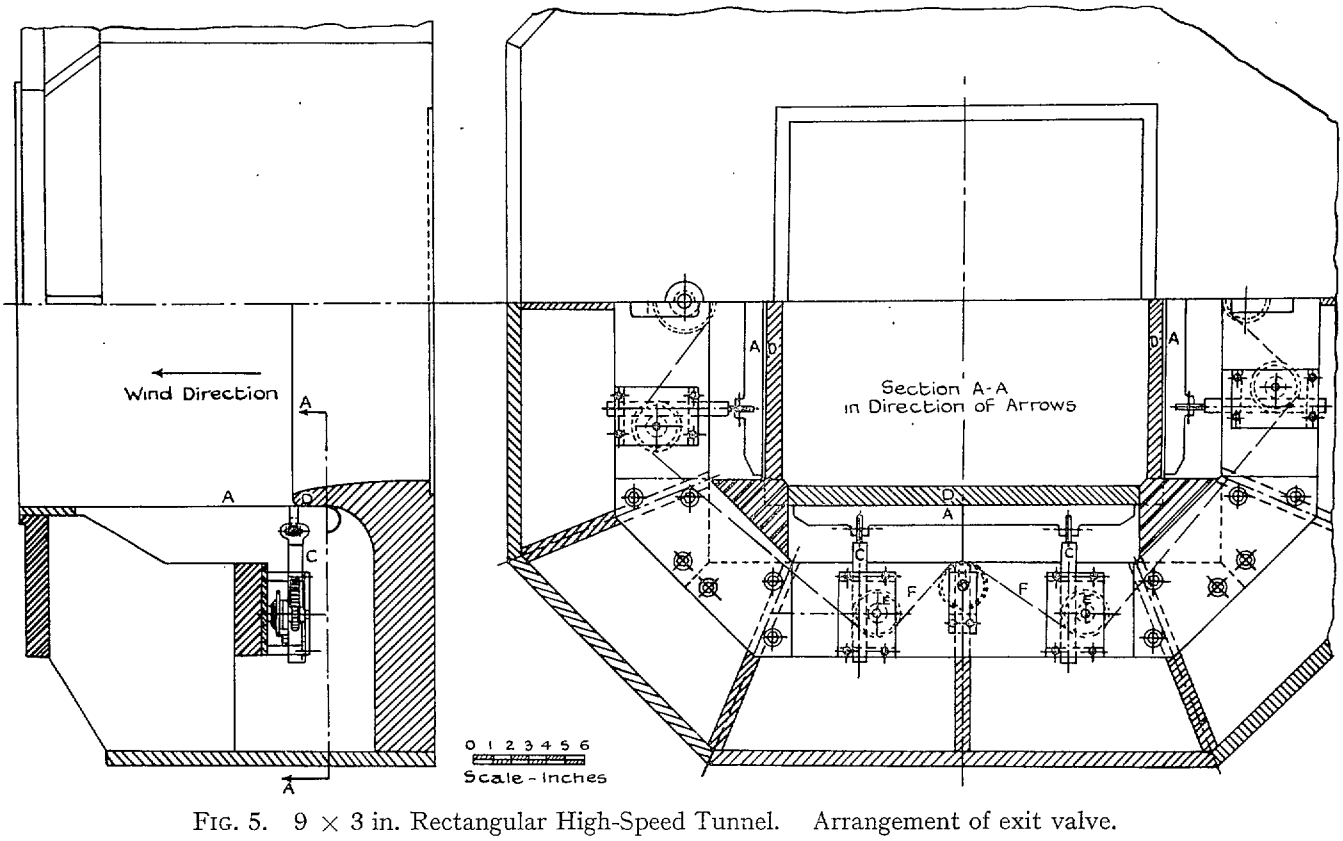

FIG. 5. 9 × 3 in. Rectangular High-Speed Tunnel. Arrangement of exit valve.

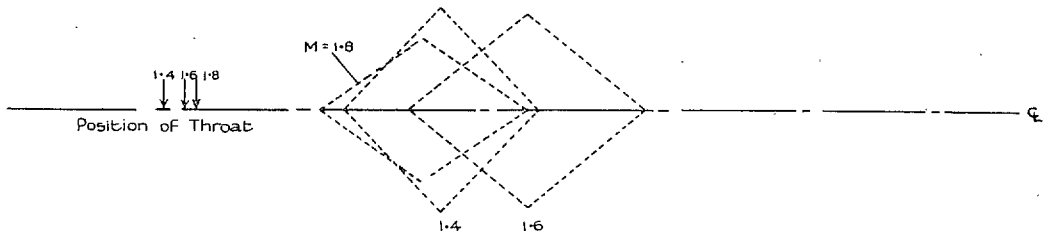

(a) Shapes and Positions of Test Diamonds (Regions of Constant M)

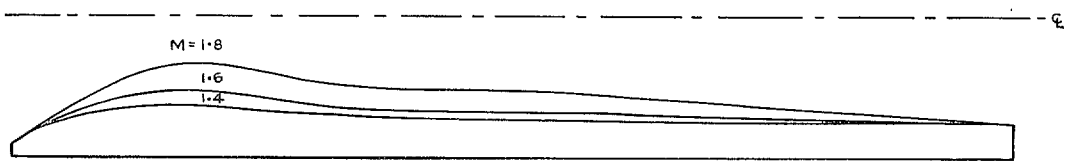

(b) Liner Shapes

FIG. 6. Liners for supersonic operation.

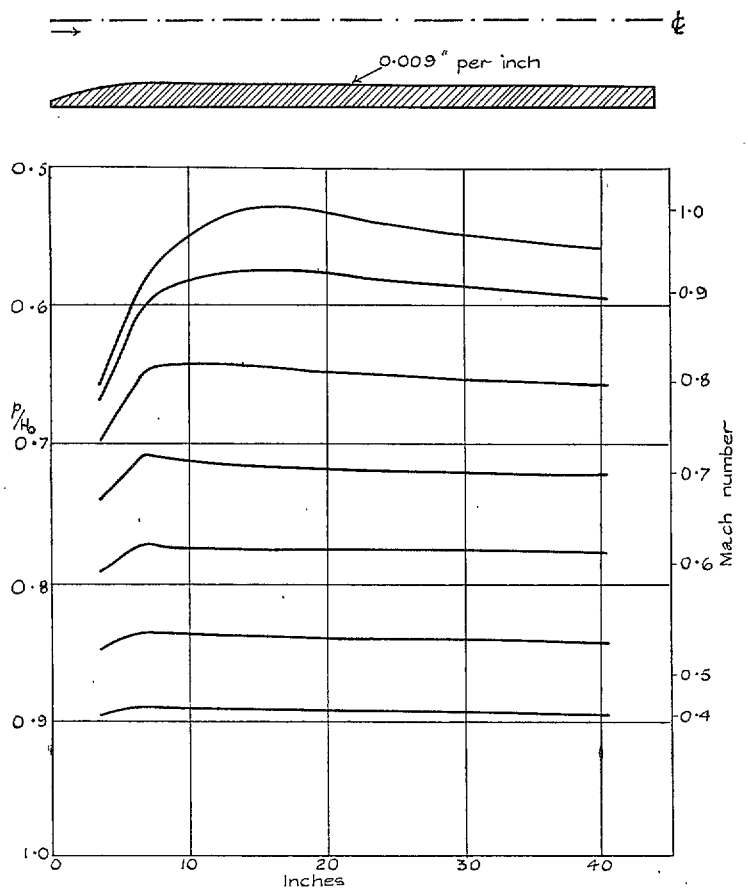

FIG. 7. Pressure distributions along subsonic liners.

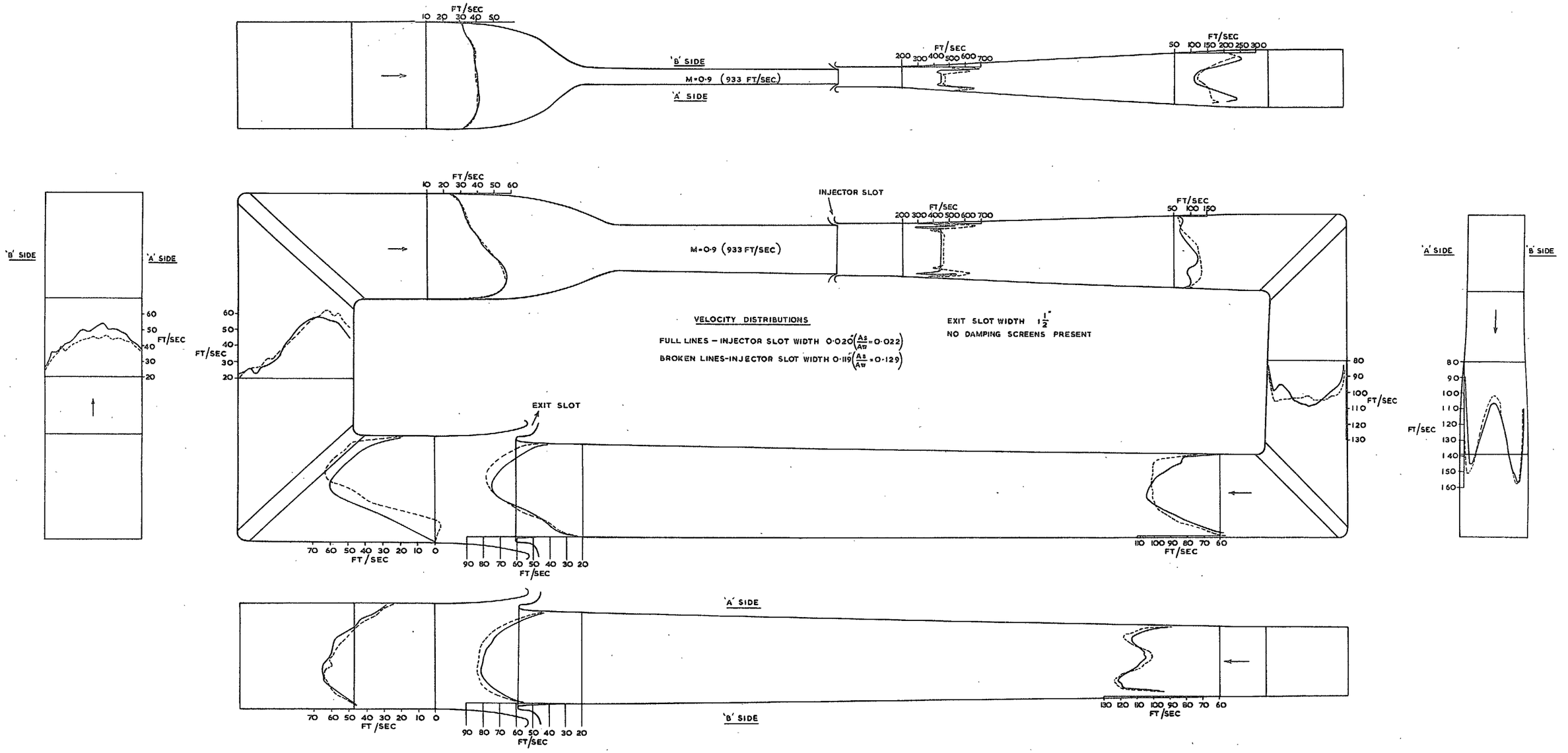

FIG. 8. VELOCITY DISTRIBUTION IN CIRCUIT OF 9"x 3" TUNNEL AT M=0·9

4801

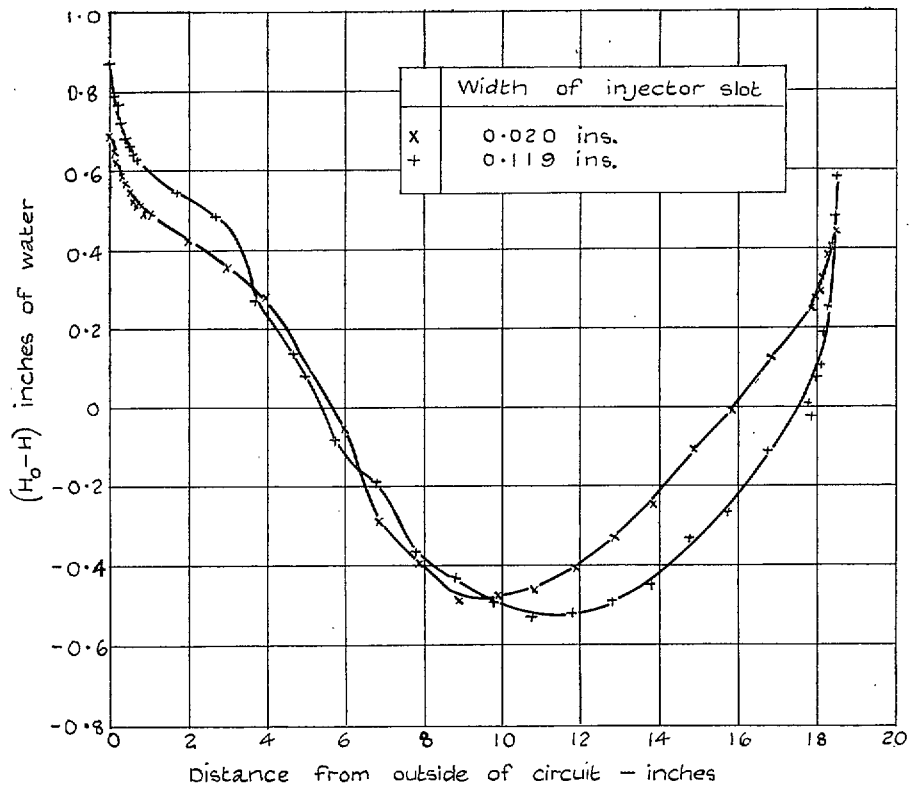

FIG. 9. Variation of total head across tunnel upstream of exit valve.

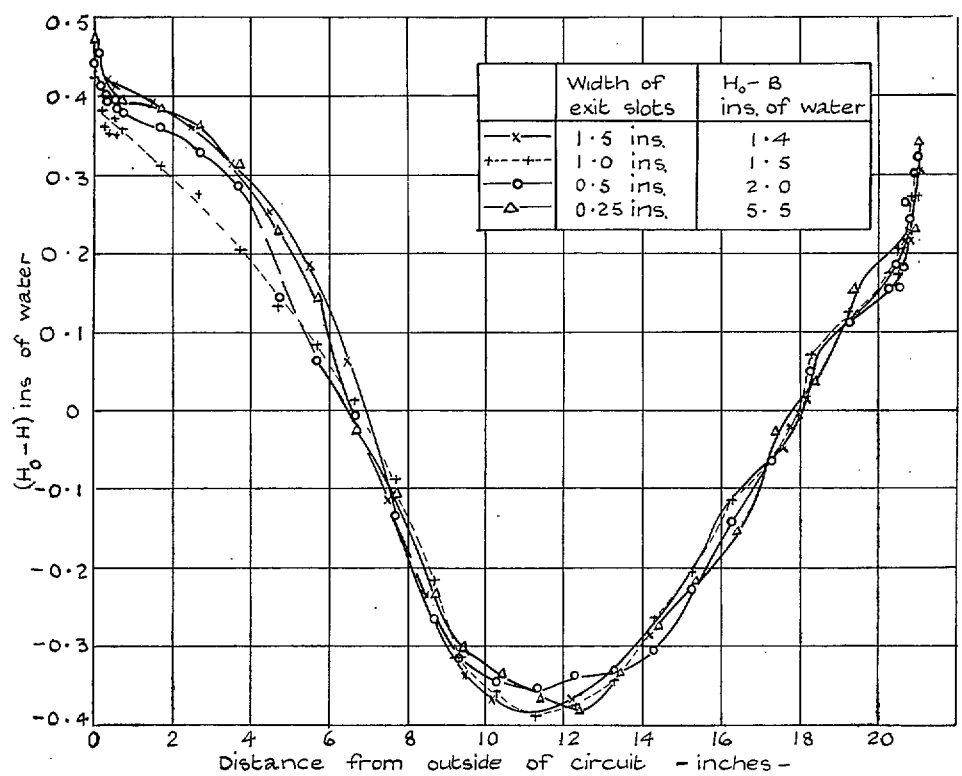

FIG. 10. Variation of total head across tunnel downstream of exit valve.
Injector slot width = 0·020 in. ($A_S/A_W = 0·022$).

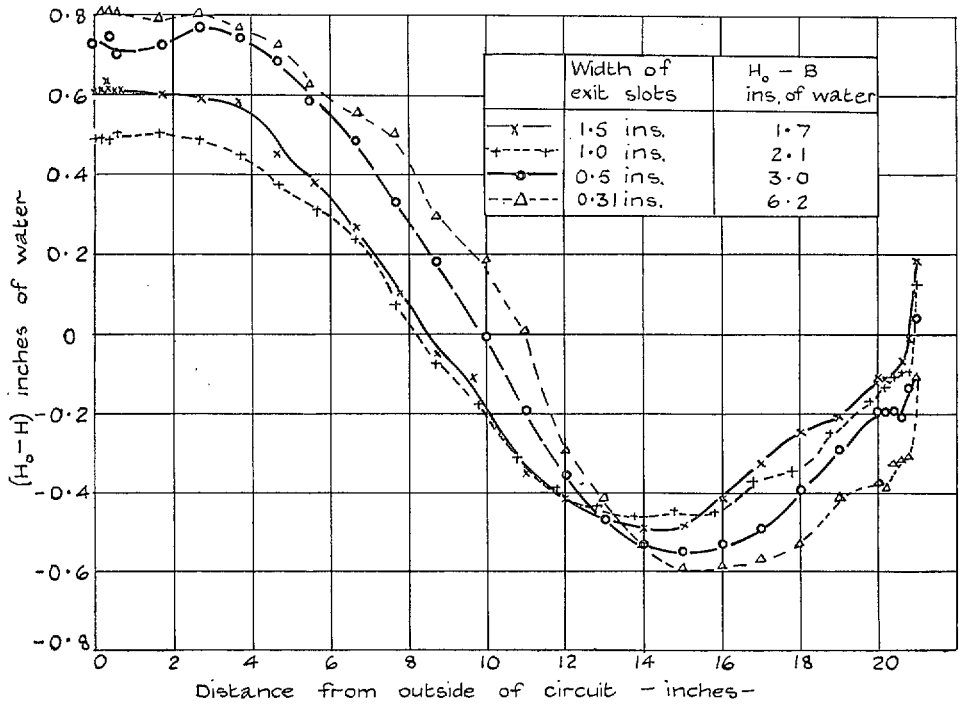

FIG. 11. Variation of total head across tunnel downstream of exit valve. Injector slot width = 0·119 in. ($A_S/A_W = 0·129$).

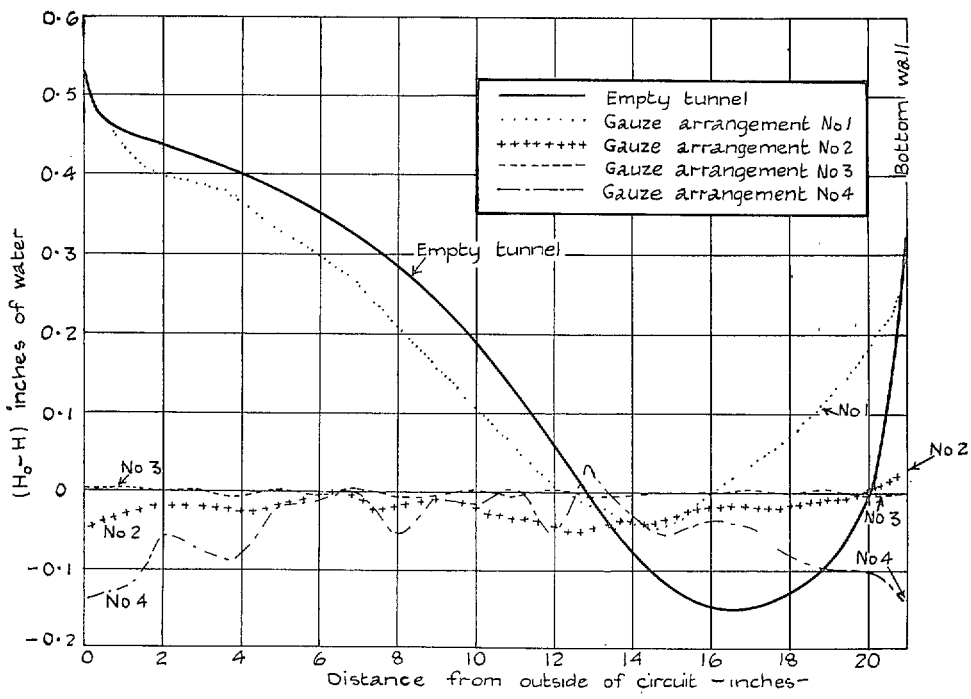

FIG. 12. Variation of total head across tunnel upstream of contraction at $M = 0·9$.

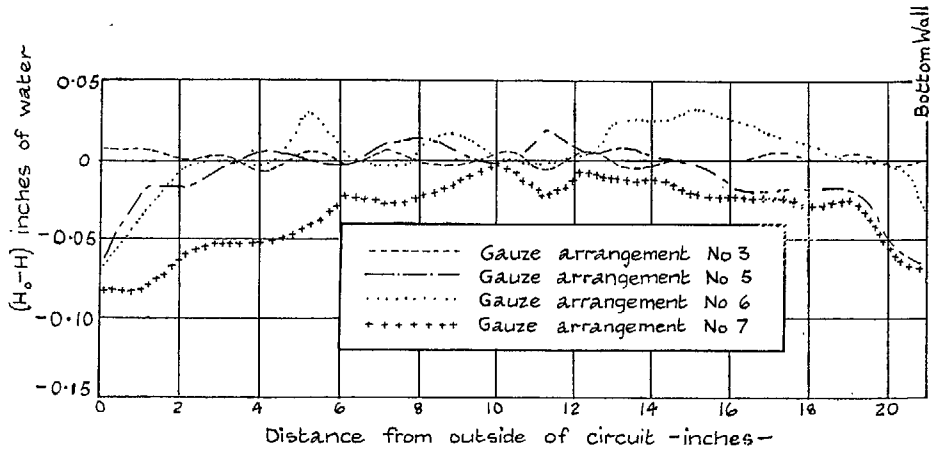

FIG. 13. Variation of total head across tunnel upstream of contraction at $M = 0{\cdot}9$.

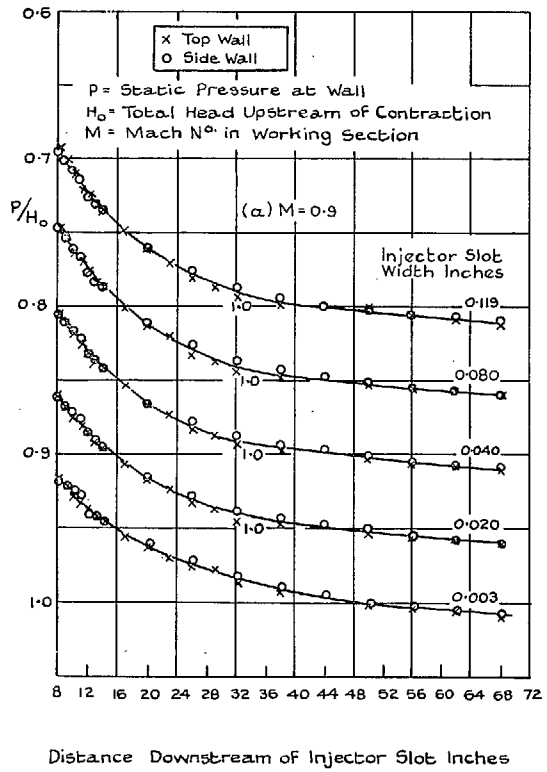

FIG, 14a. Pressure distribution along diffuser.

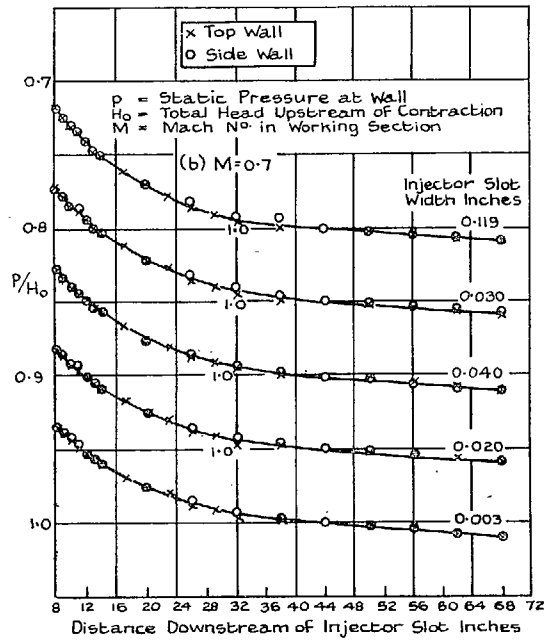

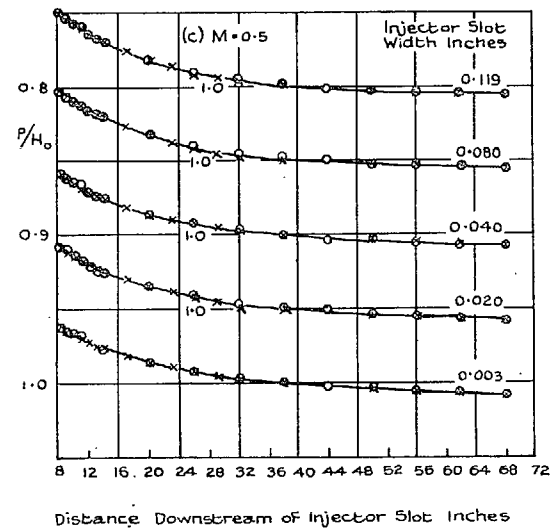

FIGS. 14b and 14c. Pressure distribution along diffuser.

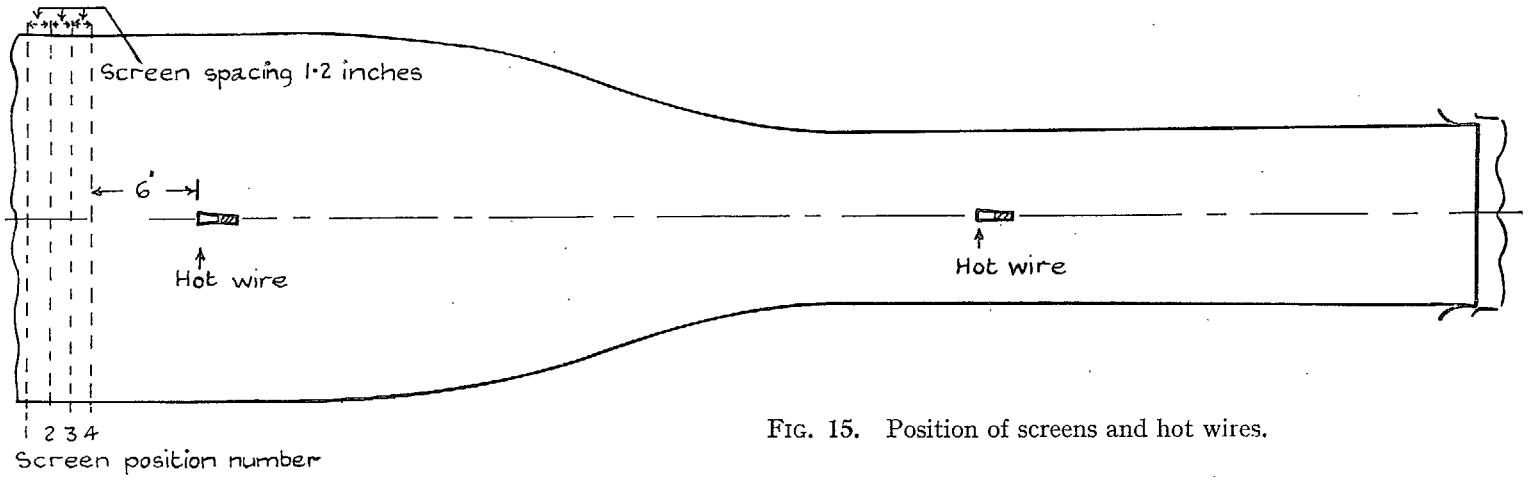

FIG. 15. Position of screens and hot wires.

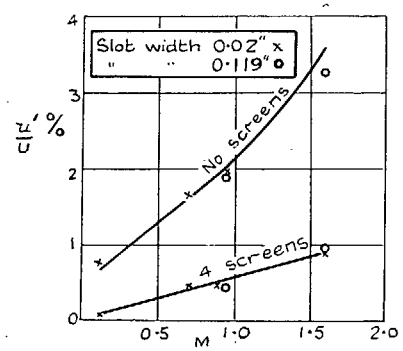

FIG. 16. Variation of turbulence upstream of contraction with working-section Mach number.

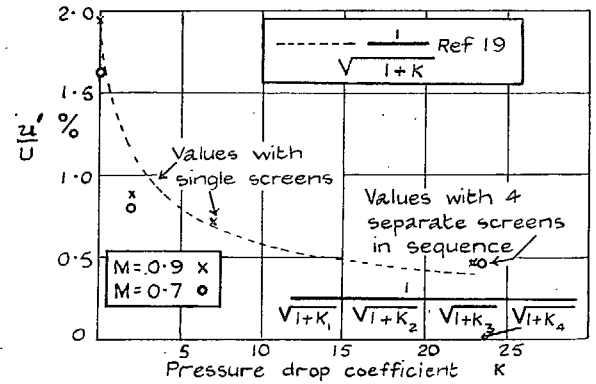

FIG. 17. Variation of turbulence upstream of contraction with total pressure-drop coefficient of screens.

(24217) Wt. 15-680 K9 10/53 F. M. & S.

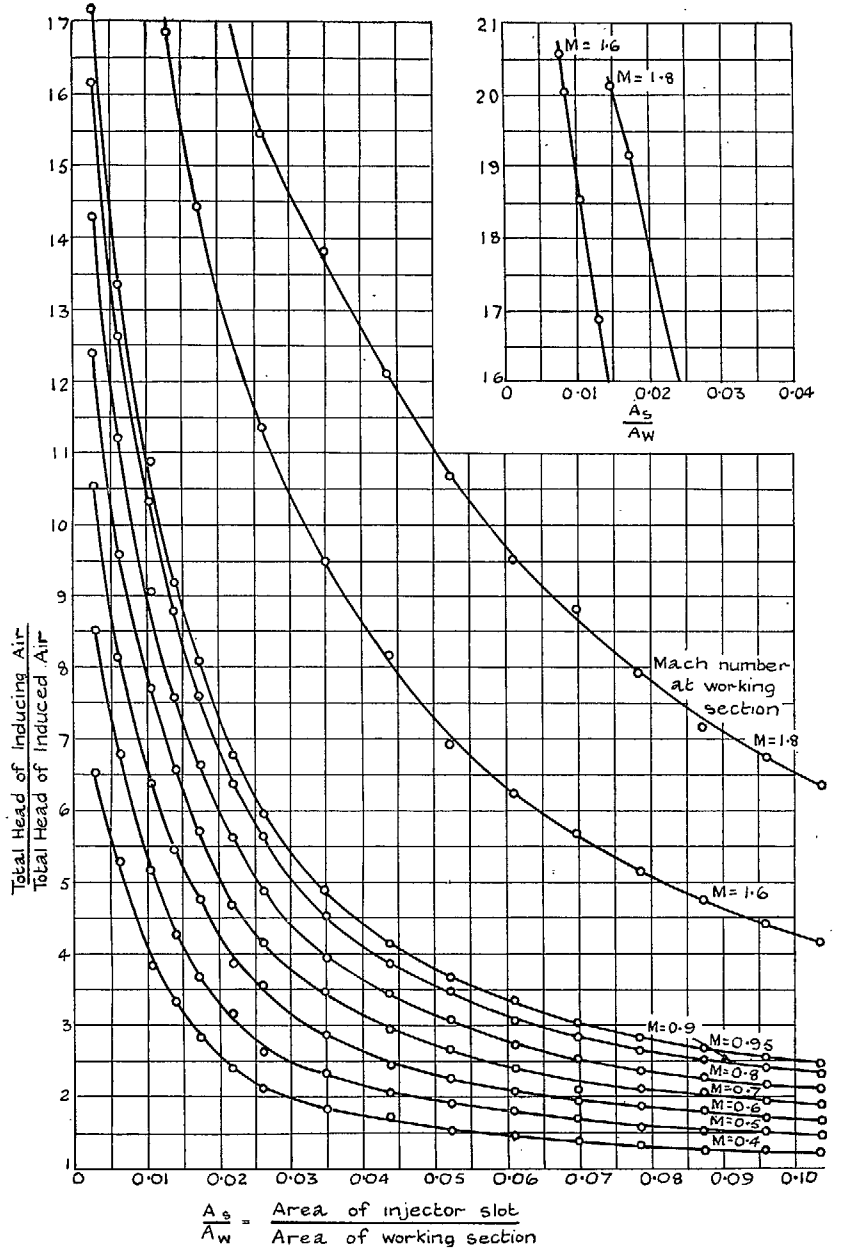

FIG. 18. Blowing pressure as a function of slot area and Mach number.

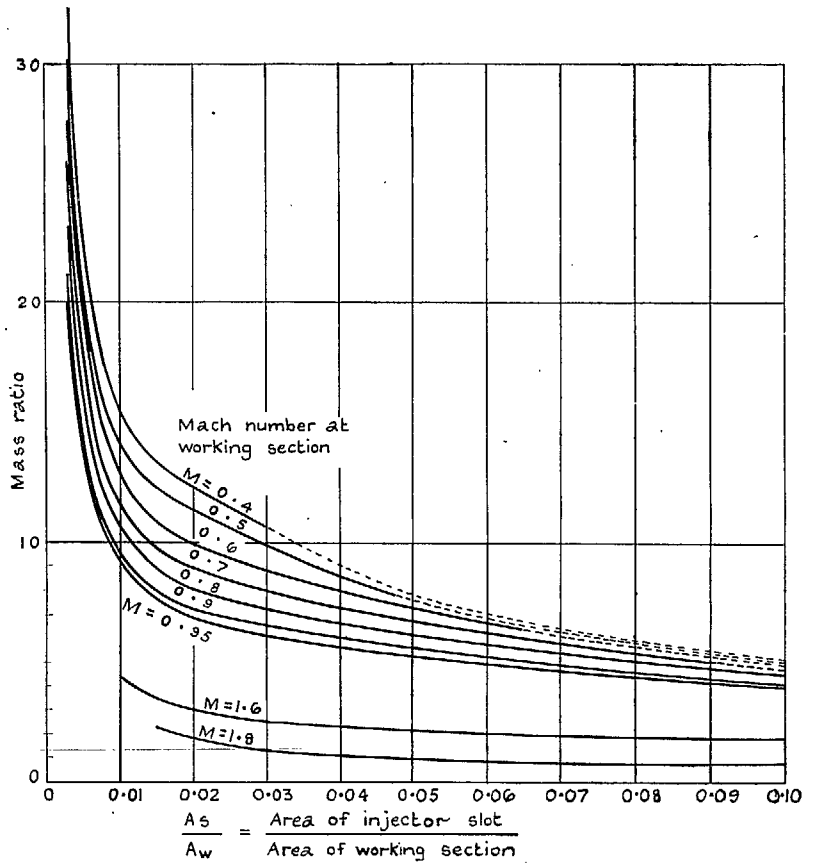

Fig. 19. Mass ratio as a function of slot area and Mach number.

PRINTED IN GREAT BRITAIN

Publications of the Aeronautical Research Council

ANNUAL TECHNICAL REPORTS OF THE AERONAUTICAL RESEARCH COUNCIL (BOUND VOLUMES)

1936 Vol. I. Aerodynamics General, Performance, Airscrews, Flutter and Spinning. 40*s.* (40*s.* 9*d.*)
Vol. II. Stability and Control, Structures, Seaplanes, Engines, etc. 50*s.* (50*s.* 10*d.*)

1937 Vol. I. Aerodynamics General, Performance, Airscrews, Flutter and Spinning. 40*s.* (40*s.* 10*d.*)
Vol. II. Stability and Control, Structures, Seaplanes, Engines, etc. 60*s.* (61*s.*)

1938 Vol. I. Aerodynamics General, Performance, Airscrews. 50*s.* (51*s.*)
Vol. II. Stability and Control, Flutter, Structures, Seaplanes, Wind Tunnels, Materials. 30*s.* (30*s.* 9*d.*)

1939 Vol. I. Aerodynamics General, Performance, Airscrews, Engines. 50*s.* (50*s.* 11*d.*)
Vol. II. Stability and Control, Flutter and Vibration, Instruments, Structures, Seaplanes, etc. 63*s.* (64*s.* 2*d.*)

1940 Aero and Hydrodynamics, Aerofoils, Airscrews, Engines, Flutter, Icing, Stability and Control, Structures, and a miscellaneous section. 50*s.* (51*s.*)

1941 Aero and Hydrodynamics, Aerofoils, Airscrews, Engines, Flutter, Stability and Control, Structures. 63*s.* (64*s.* 2*d.*)

1942 Vol. I. Aero and Hydrodynamics, Aerofoils, Airscrews, Engines. 75*s.* (76*s.* 3*d.*)
Vol. II. Noise, Parachutes, Stability and Control, Structures, Vibration, Wind Tunnels. 47*s.* 6*d.* (48*s.* 5*d.*)

1943 Vol. I. (In the press.)
Vol. II. (In the press.)

ANNUAL REPORTS OF THE AERONAUTICAL RESEARCH COUNCIL—

1933-34 1*s.* 6*d.* (1*s.* 8*d.*)
1934-35 1*s.* 6*d.* (1*s.* 8*d.*)
April 1, 1935 to Dec. 31, 1936. 4*s.* (4*s.* 4*d.*)
1937 2*s.* (2*s.* 2*d.*)
1938 1*s.* 6*d.* (1*s.* 8*d.*)
1939-48 3*s.* (3*s.* 2*d.*)

INDEX TO ALL REPORTS AND MEMORANDA PUBLISHED IN THE ANNUAL TECHNICAL REPORTS AND SEPARATELY—

April, 1950 - - - - - R. & M. No. 2600. 2*s.* 6*d.* (2*s.* 7½*d.*)

AUTHOR INDEX TO ALL REPORTS AND MEMORANDA OF THE AERONAUTICAL RESEARCH COUNCIL—

1909-1949 - - - - - R. & M. No. 2570. 15*s.* (15*s.* 3*d.*)

INDEXES TO THE TECHNICAL REPORTS OF THE AERONAUTICAL RESEARCH COUNCIL—

December 1, 1936—June 30, 1939. R. & M. No. 1850. 1*s.* 3*d.* (1*s.* 4½*d.*)
July 1, 1939—June 30, 1945. R. & M. No. 1950. 1*s.* (1*s.* 1½*d.*)
July 1, 1945—June 30, 1946. R. & M. No. 2050. 1*s.* (1*s.* 1½*d.*)
July 1, 1946—December 31, 1946. R. & M. No. 2150. 1*s.* 3*d.* (1*s.* 4½*d.*)
January 1, 1947—June 30, 1947. R. & M. No. 2250. 1*s.* 3*d.* (1*s.* 4½*d.*)
July, 1951. - - - - - R. & M. No. 2350. 1*s.* 9*d.* (1*s.* 10½*d.*)

Prices in brackets include postage.

Obtainable from

HER MAJESTY'S STATIONERY OFFICE

York House, Kingsway, London, W.C.2; 423 Oxford Street, London, W.1 (Post Orders: P.O. Box 569, London, S.E.1); 13a Castle Street, Edinburgh 2; 39 King Street, Manchester 2; 2 Edmund Street, Birmingham 3; 1 St. Andrew's Crescent, Cardiff; Tower Lane, Bristol 1; 80 Chichester Street, Belfast or through any bookseller.

S.O. Code No. 23-2781